

Resonant nonlinear quantum transport for a periodically kicked Bose condensate

Sandro Wimberger, Riccardo Mannella, Oliver Morsch, and Ennio Arimondo
INFN, Dipartimento di Fisica E. Fermi, Università di Pisa, Largo Pontecorvo 3, 56127 Pisa, Italy

Our realistic numerical results show that the fundamental and higher-order quantum resonances of the δ -kicked rotor are observable in state-of-the-art experiments with a Bose condensate in a shallow harmonic trap, kicked by a spatially periodic optical lattice. For stronger confinement, interaction-induced destruction of the resonant motion of the kicked harmonic oscillator is predicted.

PACS numbers: 03.75.Lm, 02.70.Bf, 05.60.Gg, 32.80.-t

Dynamical systems that exchange significant energy with an external driving (time-dependent) field are paradigmatic objects for the study of complex evolutions with only a few degrees of freedom. In contrast to autonomous systems, where chaotic behavior can originate from many-body interactions, the complexity in driven systems arises from and can be controlled by the external field. An experimental setup where *both* types of complexity – many-body dynamics and external drive – are present is realizable and to a large degree controllable with state-of-the-art atom optical systems [1, 2]. Good control over nontrivial dynamics is the necessary tool for manipulating quantum states in a desired way [3]. Controlled coherent evolution is the necessary ingredient for quantum computing schemes, and, in particular, for algorithms which are based on a fast spreading over the Hilbert space of interest. Recently, ballistic expansion (i.e., linearly increasing momenta with time) was proposed to realize such quantum random walk algorithms [4].

In this Letter, we answer the question of whether ballistic resonant quantum transport can be realized with a periodically kicked Bose condensate. Cold dilute atomic gases have so far been used to realize many features of quantum chaos, such as dynamical localization [5] or dynamical tunneling [6]. To implement a fast spreading in momentum space, one can use quantum accelerator modes found recently [7], or the standard δ -kicked rotor (KR) which shows ballistic motion at the so-called quantum resonances [8]. The latter, however, are hard to realize if the initial conditions cannot be optimally controlled [9]. The preparation of a Bose condensate within harmonic traps offers very well-defined initial momenta, necessary for observing ballistic motion for a substantial number of kicks.

We use the time-dependent Gross-Pitaevskii equation (GPE) [10] to describe a Bose-Einstein condensate in an harmonic confinement which is subject to a temporally and spatially periodic optical potential, created by a far detuned optical lattice. If the external potentials are not too strong, the GPE provides a good approximation of experiments with dilute Bose gases [11, 12]. The GPE

which we numerically integrate has the following form:

$$i\hbar \frac{\partial \psi(\vec{r}, t)}{\partial t} = \left[-\frac{\hbar^2 \nabla^2}{2M} + \frac{M\omega_r^2 x^2}{2} + \frac{M\omega_r^2 \rho^2}{2} + V_0 \cos(2k_L x) \right. \\ \left. \times \sum_{m=-\infty}^{+\infty} F(t - mT) + gN |\psi(\vec{r}, t)|^2 \right] \psi(\vec{r}, t), \quad (1)$$

with $\rho^2 = y^2 + z^2$. $\psi(\vec{r}, t)$ represents the condensate wave function, and M is the atomic mass. The nonlinear coupling constant is given by $g = 4\pi\hbar^2 a/M$, N is the number of atoms in the condensate, a the s-wave scattering length, and k_L is the wave vector of the laser creating the optical potential. In principle, an arbitrary pulse shape $F(t)$ may be realized, but here we restrict ourselves to a situation where the laser is switched on at time instants separated by T , with maximum amplitude V_0 and periodic pulse shape function $F(t)$ of unit amplitude and duration $\delta T \ll T$. Our system is then the nonlinear analogue of noninteracting cold atom experiments [5, 9], which implement the KR model, and we can directly compare our results with the well-studied KR (for $\omega_x \rightarrow 0$), or with the Kicked Harmonic Oscillator (KHO) [13] (for non-vanishing ω_x). The commonly used dimensionless kick strength and kick period of the KR are $k = (V_0/\hbar) \int_0^T dt F(t)$ and $\tau = 8TE_R/\hbar$, with the recoil energy $E_R = (\hbar k_L)^2/2M$ [9].

The GPE was numerically integrated using a finite difference propagator, adapted by a predictor-corrector loop to reliably evaluate the nonlinear interaction [14]. The external, time-dependent potential makes the integration challenging, in both time and computer memory. Typical integration times range from a few hours for a simplified 1D version of Eq. (1), to several weeks for the full 3D problem. For the 1D model, the motion is confined to the longitudinal (x) direction, and we use the renormalized nonlinear coupling parameter $g_{1D} = 2\hbar\omega_r a$, assuming a radial trapping frequency $\omega_r \gg \omega_x$ [15]. Experimentally, such a confinement is obtained using a cigar-shaped optical tube, as realized in the experiment of Moritz *et al.* [16]. The initial state inserted into (1) is the relaxed condensate wave function corresponding to the *experimental ground state* in a magnetic or optical trap. The ground state lies between the cases of a Gaussian, for $g = 0$, and the Thomas-Fermi limit, which is essentially an inverted parabola, for large nonlinearity [10]. Its characteristic width σ_{p_x} in momentum space is determined by the non-

linearity. Increasing the nonlinearity in Eq. (1) leads to a smaller width σ_{p_x} of the initial state [10].

The dynamics of the system described by (1) depends sensitively on the relative strength of the three potentials, i.e., on the control parameters V_0 (for fixed pulse shape), ω_x , and g . Since the system absorbs energy from the optical lattice, we must at all times compare the kinetic energy with the (longitudinal) trap potential and the nonlinear term. If the latter two contributions are small, we can easily realize ballistic quantum motion, up to interaction times above which the trap potential is no longer negligible. On the other hand, we can tune the system to a situation where the trap crucially affects the dynamics, and we then have a realization of the KHO.

In the following, we show that the fundamental as well as higher-order quantum resonances (QR) of the KR can be observed in an experiment using a Bose condensate, in the presence of a shallow harmonic confinement. In the linear KR, the QRs occur at specific kick periods $T = T_T s/r$ (s, r integer) [8]. At the Talbot time $T = T_T$, the amplitudes of the wave function in momentum space exactly rephase between successive kicks for particular initial momenta ($p_{\text{init}} = 0$) [1, 8]. The result is a maximal, i.e., perfectly phase-matched, absorption of energy from the kicks, leading to a ballistic spread of the wave packet [8, 9]. Only signatures of the QRs at $T = T_T/2$ and $T = T_T$ have been observed up to now in experiments with essentially non-interacting atoms, because the initial momenta of the atoms could not be sufficiently controlled [9].

Figure 1 presents our results for the fundamental QR of the KR at the Talbot time for Rb atoms, $T = T_T = \pi\hbar/(2E_R) \simeq 66.26 \mu\text{s}$, with $k_L \simeq 8.1 \times 10^6 \text{ m}^{-1}$. Shown are the kinetic energy and the momentum distribution of the condensate along the longitudinal direction. The energy is computed from the momentum distribution, integrated over the transverse directions, i.e.,

$$E(K) = \frac{1}{2} \int dp_x p_x^2 P(p_x, K)$$

with $P(p_x, K) \equiv \int dp_y dp_z |\psi(\vec{p}, t = KT)|^2$, (2)

where K denotes the number of kicks. We present also the integrated spatial distribution along the transverse direction [in y , or equivalently z , because of the radial symmetry in Eq. (1)]: $P_y(K) = \int dx dz |\psi(\vec{r}, t = KT)|^2$. As an example for higher-order QRs, which up to now have never been resolvable experimentally, Fig. 2 shows data for the resonance at $T = T_T/4$. For all the parameters studied, the ballistic quantum transport, with a quadratic growth $E(K) \propto K^2$, is clearly visible.

Deviations from the idealized ballistic motion arise because of the contributions of the trap potential and the nonlinearity. At long times, the expanding condensate feels the harmonic trap potential, and further acceleration is hindered by the trap. This effect is negligible for

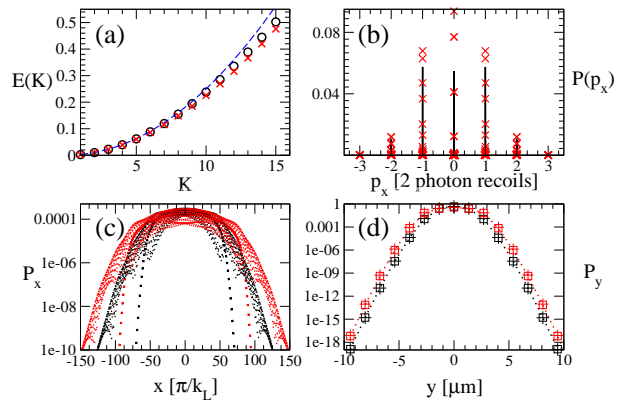


FIG. 1: (color online). (a) Kinetic energy (in units of $8E_R$) vs K , at $T = T_T$, $k = 0.1$ (pulse width $\delta T \simeq 500$ ns, rise time 70 ns; $V_0/E_R \simeq 8$), $\omega_x/2\pi = 10$ Hz, $\omega_r/2\pi = 100$ Hz, and $N = 10^4$ (circles), $N = 5 \times 10^4$ (crosses). The linear KR evolution with $p_{\text{init}} = 0$ is shown by the dashed line. (b) Momentum distribution (2) after $K = 15$, $N = 10^4$ (solid line), $N = 5 \times 10^4$ (crosses). (c) The longitudinal (dotted line: $K = 0$; shaded area: $K = 15$) and (d) the transverse (dotted line: $K = 0$; squares: 7; pluses: 15) spatial distributions for $N = 10^4$ (thinner distributions) and $N = 5 \times 10^4$ (broader distributions). The transverse dynamics is frozen due to the small effective nonlinearity.

vanishing ω_x . Equating the longitudinal trap potential and the kinetic energy, and using $p_x \lesssim \pi k K \hbar k_L$ at $T = T_T$ [8, 17], we estimate the kick number above which the trap dominates the dynamics as $K \sim 2k_L \sqrt{\hbar/M\omega_x} \simeq 55$ for the parameters of Fig.1. More crucial is the small but finite initial condensate momentum spread ($\sigma_{p_x} \ll 2\hbar k_L$ [1, 2]), which, after a characteristic time $t^* \propto 1/\sigma_{p_x}$, leads to a linear increase of the energy $E(K) \propto K$ [17]. This crossover sets in at $K \simeq 10$ in Fig. 1 (a). For small σ_{p_x} , the condensate ground state extends over many lattice sites of the kick potential, which in turn makes a smaller trap potential necessary for ideal ballistic motion. The interplay between these situations is illustrated in Fig. 3, where we systematically vary the number of atoms in the condensate. We stress that the effect of the nonlinearity manifests itself indirectly via its influence on the initial state, while the nonlinear interaction is negligible during the kick evolution. This finding is quite surprising, remembering that the QRs correspond to exact phase revivals between kicks. On short time scales, however, the perturbation induced by the nonlinearity cannot accumulate a large enough dephasing, because even for the small kick strength $k < 0.5$ it is at least 1 order of magnitude smaller than the kinetic energy. Our results are consistent with a simplified 1D model analysis of the QR, in the presence of a small nonlinear perturbation [18]. This analysis, however, could not account for the exact nonlinear wave packet evolution including the harmonic confinement.

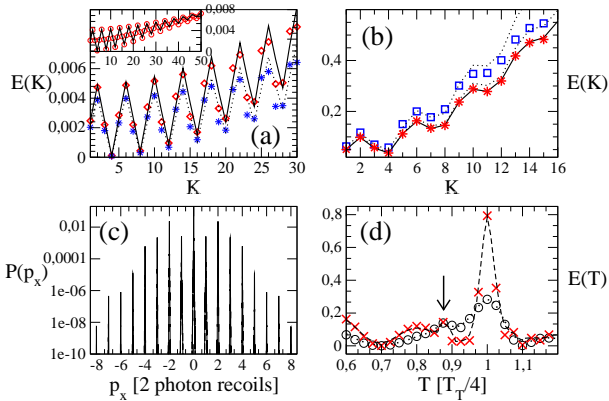


FIG. 2: (color online). Kinetic energies at $T = T_T/4$, same trap and pulse shape as in Fig. 1: (a) 1D, $N = 10^4$, $k = 0.1$ (red diamonds) and $k = 0.09$ (blue stars), and (b) $k = 0.45$ ($V_0/E_R \simeq 42$), $N = 10^4$ (1D, solid line; 3D red stars), and 3D $k = 0.48$ ($V_0/E_R \simeq 45$), $N = 10^3$ (squares). (c) Momentum distribution (2) for 3D with $k = 0.45$ after $K = 15$. (d) A scan of the kinetic energy vs T for the 1D case from (b), after $K = 10$ (circles) and $K = 20$ (red crosses), with the corresponding data for the linear KR (dotted and dashed lines). The resonance at $T = T_T/4$ manifests itself clearly, and a tiny peak of another higher-order resonance is marked by the arrow. The inset in (a) confirms the correspondence between our method (circles) and a 1D fast Fourier transform evolution of the linear KR (solid line) [a wave packet (circles) or an incoherent ensemble of plane waves (solid line) was evolved respectively, with initial Gaussian momentum distribution – $\sigma_{p_x} = 0.026 \hbar k_L - k = 0.09$]. For comparison, the linear KR ($p_{\text{init}} = 0$) in (a) for $k = 0.1$ (solid line), $k = 0.09$ (dotted line), and (b) $k = 0.48$, $k = 0.45$ (dotted line).

We finally note that for a large number of atoms $N \geq 5 \times 10^4$ the results of our 1D model and the full 3D computations differ [c.f. Fig. 3(a)] because initially the condensate substantially expands along the transverse directions. This is crucial for the realization of ballistic quantum transport, since for the same number of atoms in the condensate, the trap has less effect in the 3D as compared with the 1D case, but, on the other hand, σ_{p_x} in the 3D case is slightly larger. For the parameters of Fig. 3(a), the larger σ_{p_x} has a negligible influence, while the smaller initial spatial extension allows the ballistic motion to survive longer in the 3D than in the 1D case.

The nonlinearity manifests itself if we scan the kick period over the fundamental QR and plot the kinetic energy at fixed K . The resonance peak shows a slight asymmetry, which does not occur in the linear KR. The asymmetry decreases when (i) reducing the longitudinal confinement [solid line as compared with circles in Fig. 4(a)], or (ii) evolving the initial condensate state without the nonlinear term [pyramids in Fig. 4(a)]. Again the trap potential hides the influence of the nonlinearity, but the observed asymmetry originates from both perturbations of the usual KR. Any such perturbation is

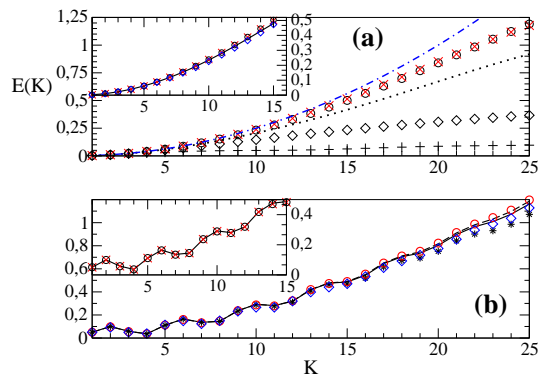


FIG. 3: (color online). Scan of the number of atoms (trap as in Fig.1 if not stated otherwise): (a) for $T = T_T$, and 1D $N = 5 \times 10^3$ (crosses), $N = 10^4$ (circles) $N = 5 \times 10^4$ (diamonds), $N = 10^5$ (plusses); 3D in the inset for $N = 10^3$ (solid line), $N = 5 \times 10^3$ (crosses), $N = 10^4$ (circles) $N = 5 \times 10^4$ (diamonds). The dot-dashed line shows the analytical result $E(K) = k^2 K^2/4$ [linear KR, $p_{\text{init}} = 0$], and the dotted line 1D data for $\omega_x/2\pi = 5$ Hz, and $N = 5 \times 10^4$. (b) $T = T_T/4$, $k = 0.45$, 1D for $N = 10^2$ (stars), $N = 10^3$ (solid line), $N = 3 \times 10^3$ (dashed), $N = 10^4$ (circles), $N = 5 \times 10^4$ (diamonds); 3D in the inset for $N = 10^3$ (solid line), $N = 5 \times 10^3$ (crosses), $N = 10^4$ (circles).

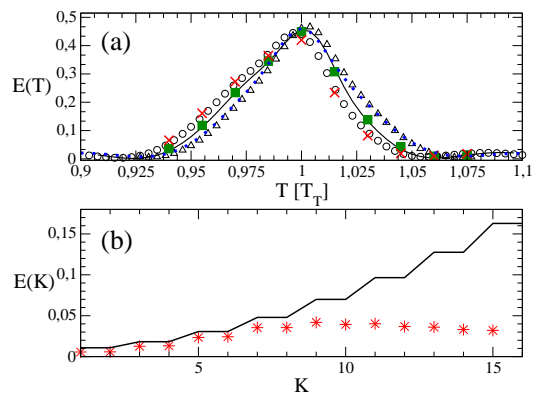


FIG. 4: (color online). (a) Scan of the kinetic energy vs T around $T = T_T$, parameters as in Fig. 1, in comparison with the linear KR (blue dots; $\sigma_{p_x} = 0.01 \hbar k_L$), after $K = 14$; 1D ($N = 10^4$: circles; $\omega_x/2\pi = 5$ Hz: solid line; $N = 0$ in kick evolution: pyramids), and 3D ($N = 10^4$: green squares; $N = 5 \times 10^4$: red crosses). (b) Kinetic energy of 3D KHO with $T = 250 \mu\text{s}$, $\omega_x/2\pi = 1$ kHz, $\omega_r/2\pi = 5$ kHz, and $k = 0.1$ for $N = 0$ (solid line) and $N = 100$ (stars).

expected to introduce an asymmetric peak shape, following a semiclassical analysis specifically developed for the description of decoherence by spontaneous emission [17].

We can also tune our system described by the GPE (1) to the limit, in which the nonlinear interaction term becomes very important and even dominant for small kick strength. Experimentally such a situation can be realized either close to a Feshbach resonance (where the scattering length for two-body atomic collisions can increase

by orders of magnitude [10]) or by simply increasing the strength of the harmonic confinement. The latter situation has been analysed as a nonlinear generalization of the KHO in [11, 19]. The analysis showed clear signatures of the nonlinearity in the resonant transport regime of the KHO, i.e., for $T\omega_x = 2\pi/r$ with $r = 3, 4, 6$, where the quantum transport is enhanced with respect to the classical one, much in the same way as at the QRs of the KR [13]. In the KR studied above, the total energy – corresponding to the chemical potential in the stationary case [10] – is almost entirely given by the kinetic energy obtained from the kicks. In the KHO, the energy distribution is very different: here the kinetic, the potential, and the self energy (given by the nonlinear term) are of the same order of magnitude, which leads to a nonlinearity-induced redistribution of energy also to the transverse degrees of freedom.

Our numerical technique can be used to generalize the previous studies of the nonlinear KHO to the full 3D GPE, properly including the coupling of the transverse dimensions which is necessary for comparison with real-life experiments. Results on the KHO are presented in Fig. 4(b), where we observe the destruction of the resonant motion at $T\omega_x = \pi/2$ already for a small number of atoms $N = 100$, and after just a few kicks. In contrast to what was done in [11, 19], the initial state need not be translated away from the classically stable origin in phase space. It suffices to use the relaxed ground state of the condensate to observe the impact of the now much stronger effective nonlinearity due to the strong harmonic confinement.

We have tested our data in different ways, making sure that our numerical codes produce stable results. In the 1D case and for $g_{1D} = 0$, we compared them either with analytical results for the linear KR [8], or with the much simpler evolution on a discrete grid, using a standard fast Fourier transform (FFT) [17, 18]. The analytic growth rate of the kinetic energy for $p_{\text{init}} = 0$ at $T = T_T$ is shown in Fig. 1(a). For $T = T_T/4$, in the inset of Fig. 2(a), we compare both evolutions for up to $K = 50$ kicks. The FFT code does not take into account (i) the trap, (ii) the finite duration of the pulses, and (iii) the coherent evolution of the wave packet, which explains the tiny deviations for $K \geq 40$. The damping of the oscillations is due to the nonzero σ_{p_x} , an effect which was experimentally observed also for the anti-resonance $T = T_T/2$ in [2], where the motion of the linear KR is perfectly periodic only for $p_{\text{init}} = 0$.

In summary, we presented the first (3+1) dimensional treatment of a Bose condensate driven by an external temporally periodic force, which controls the dynamics of the system. Ballistic motion is shown to be realizable

over a substantial number of kicks, even in the presence of a weak harmonic confinement. Within the framework of the 3D GPE, we have taken a first step towards the study of higher-dimensional chaos induced by the nonlinear coupling of the spatial dimensions, and future work will concentrate on situations where the transverse degrees of freedom significantly contribute to the dynamics.

This work was supported by MIUR, COFIN-2004, the Humboldt Foundation (Feodor-Lynen Program), the Scuola di Dottorato G. Galilei, and the ESF (CATS).

-
- [1] L. Deng *et al.*, Phys. Rev. Lett. **83**, 5407 (1999).
 - [2] G.J. Duffy, A.S. Mellish, K.J. Challis, and A.C. Wilson, Phys. Rev. A **70**, 041602(R) (2004).
 - [3] S. Pötting, M. Cramer, and P. Meystre, Phys. Rev. A **64**, 063613 (2001); J. Gong and P. Brumer, Phys. Rev. Lett. **88**, 203001 (2002).
 - [4] See, e.g., D. K. Wójcik and J. R. Dorfman, Phys. Rev. Lett. **90**, 230602 (2003); T. A. Brun, H. A. Carteret, and A. Ambainis, *ibid.* **91**, 130602 (2003).
 - [5] M.G. Raizen, Adv. At. Mol. Opt. Phys. **41**, 43 (1999).
 - [6] D.A. Steck, W.H. Oskay, and M.G. Raizen, Science **293**, 274 (2001); W.K. Hensinger *et al.*, Nature **412**, 52 (2001).
 - [7] M.K. Oberthaler *et al.*, Phys. Rev. Lett. **83**, 4447 (1999).
 - [8] F.M. Izrailev, Phys. Rep. **196**, 299 (1990).
 - [9] W.H. Oskay *et al.*, Opt. Comm. **179**, 137 (2000); M.B. d’Arcy *et al.*, Phys. Rev. E **69**, 027201 (2004); G. Duffy *et al.*, *ibid.* **70**, 056206 (2004); S. Wimberger *et al.*, Phys. Rev. A (to be published), e-print physics/0502061.
 - [10] C.J. Pethick and H. Smith, *Bose-Einstein Condensation in Dilute Gases*, (Cambridge University Press, Cambridge, 2002); L. Pitaevskii and S. Stringari, *Bose-Einstein Condensation*, (Oxford University Press, Oxford, 2003).
 - [11] S.A. Gardiner *et al.*, Phys. Rev. A **62**, 023612 (2000).
 - [12] C. Zhang, J. Liu, M.G. Raizen, and Q. Niu, Phys. Rev. Lett. **92**, 054101 (2004); B. Mielck and R. Graham, J. Phys. A **37**, L581 (2004).
 - [13] G.M. Zaslavsky *et al.*, *Weak chaos and quasi-regular patterns* (Cambridge University Press, 1992); F. Borgonovi and L. Rebuzzini, Phys. Rev. E **52**, 2302 (1995); A.R.R. Carvalho and A. Buchleitner, Phys. Rev. Lett. **93**, 204101 (2004).
 - [14] E. Cerboneschi *et al.*, Phys. Lett. A **249**, 495 (1998).
 - [15] M. Olshanii, Phys. Rev. Lett. **81**, 938 (1998).
 - [16] H. Moritz, T. Stoferle, M. Köhl, and T. Esslinger, Phys. Rev. Lett. **91**, 250402 (2003).
 - [17] S. Wimberger, I. Guarneri, and S. Fishman, Nonlinearity **16**, 1381 (2003); Phys. Rev. Lett. **92**, 084102 (2004).
 - [18] L. Rebuzzini, S. Wimberger, and R. Artuso, Phys. Rev. E **71**, 036220 (2005).
 - [19] R. Artuso and L. Rebuzzini, Phys. Rev. E **66**, 017203 (2002).